



HAL
open science

From light-scattering measurements to polarizability derivatives in vibrational Raman spectroscopy: The 2 $\nu(5)$ overtone of SF₆

David Kremer, Florent Rachet, Michel Chrysos

► **To cite this version:**

David Kremer, Florent Rachet, Michel Chrysos. From light-scattering measurements to polarizability derivatives in vibrational Raman spectroscopy: The 2 $\nu(5)$ overtone of SF₆. *Journal of Chemical Physics*, 2013, 138 (17), Non spécifié. 10.1063/1.4803160 . hal-03344721

HAL Id: hal-03344721

<https://univ-angers.hal.science/hal-03344721>

Submitted on 15 Sep 2021

HAL is a multi-disciplinary open access archive for the deposit and dissemination of scientific research documents, whether they are published or not. The documents may come from teaching and research institutions in France or abroad, or from public or private research centers.

L'archive ouverte pluridisciplinaire **HAL**, est destinée au dépôt et à la diffusion de documents scientifiques de niveau recherche, publiés ou non, émanant des établissements d'enseignement et de recherche français ou étrangers, des laboratoires publics ou privés.

From light-scattering measurements to polarizability derivatives in vibrational Raman spectroscopy: The 2v₅ overtone of SF₆

D. Kremer, F. Rachet, and M. Chrysos

Citation: *The Journal of Chemical Physics* **138**, 174308 (2013); doi: 10.1063/1.4803160

View online: <http://dx.doi.org/10.1063/1.4803160>

View Table of Contents: <http://scitation.aip.org/content/aip/journal/jcp/138/17?ver=pdfcov>

Published by the [AIP Publishing](#)

Articles you may be interested in

[More light on the 2v₅ Raman overtone of SF₆: Can a weak anisotropic spectrum be due to a strong transition anisotropy?](#)

J. Chem. Phys. **140**, 034308 (2014); 10.1063/1.4861047

[Field-resolved measurement of reaction-induced spectral densities by polarizability response spectroscopy](#)

J. Chem. Phys. **127**, 184505 (2007); 10.1063/1.2792943

[Isotropic and anisotropic collision-induced light scattering by gaseous sulfur hexafluoride at the frequency region of the v₁ vibrational Raman line](#)

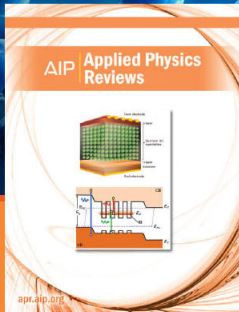
J. Chem. Phys. **118**, 11009 (2003); 10.1063/1.1575733

[The 5th- and 7th-order 2D Raman spectroscopy for intramolecular vibrational modes](#)

AIP Conf. Proc. **503**, 144 (2000); 10.1063/1.1302858

[Coherent two-dimensional Raman scattering: Frequency-domain measurement of the intra- and intermolecular vibrational interactions](#)

J. Chem. Phys. **108**, 1326 (1998); 10.1063/1.475505



NEW Special Topic Sections

NOW ONLINE
Lithium Niobate Properties and Applications:
Reviews of Emerging Trends

AIP | Applied Physics
Reviews

From light-scattering measurements to polarizability derivatives in vibrational Raman spectroscopy: The $2\nu_5$ overtone of SF_6

D. Kremer, F. Rachet, and M. Chrysos^{a)}

LUNAM Université, Université d'Angers, CNRS UMR 6200, Laboratoire MOLTECH-Anjou, 2 Bd Lavoisier, 49045 Angers, France

(Received 23 March 2013; accepted 16 April 2013; published online 7 May 2013)

The room-temperature isotropic spectrum of SF_6 was recorded at the frequency of the $2\nu_5$ overtone by running high-sensitivity incoherent Raman experiments for two independent polarizations of the incident beam and for gas densities varying from 2 to 27 amagat. Weak yet observable pressure effects were found. A transparent analysis of the Raman cross-section problem along with the first-ever prediction of the value of the mean polarizability second derivative $\partial^2\bar{\alpha}/\partial q_5^2$ are made and the hitherto underestimated role of the hot bands of SF_6 is brought to the wider public. The emergence of an analytic hotband factor is shown whose magnitude is dramatically increased with the order of the overtone and the gas temperature and all the more so upon considering low-frequency molecular vibrations. Our formulas, which in the harmonic approximation are exact, are still applicable to real situations provided certain conditions are fulfilled. For nondegenerated modes, generalization to higher order overtones is made, an issue addressing the much challenging problem of the IR-allowed second overtone bands. The content of this paper is also an invitation towards *ab initio* derivative-calculations for sulfur hexafluoride, especially given the today's needs in interpreting spectra of significance for greenhouse atmospheric issues. © 2013 AIP Publishing LLC. [<http://dx.doi.org/10.1063/1.4803160>]

I. INTRODUCTION

Vibrational Raman and IR spectroscopy in nonpolar compressed molecular gases, though among the age-old techniques, still proves the best way to access dipole polarizability and dipole moment derivatives with respect to the vibration normal coordinates of a molecule¹⁻³ (see also Refs. 4-8, and references therein). Within that spectroscopy, frequency-resolved spectra, generated by the oscillating dipole-dipole polarizability α or dipole moment μ , are recorded around the frequency of a vibrational transition, from which a lot can be learnt about the way in which the molecule oscillates at that frequency. It happens often that the absorption or scattering cross-section of a vibrational transition is too small a value to emerge from the noise, thus requiring high gas pressures to make enough intense signals appear. In doing so, however, line spectra start to overlap due to neighboring transitions, resulting in a spectrum that looks more like a broad bump than like anything described as a sharp spectral line at the expected frequency.⁹ Serious difficulties may thus appear with the interpretation. This is even more so when the equipment used to record the intensities is not designed for high resolution imaging, and spectral resolutions of the order of $\sim 1 \text{ cm}^{-1}$ are only possible. Although such values are too low a performance in comparison to some of today's feats of instrumentation,¹⁰⁻¹² it is sometimes the cost of the effort required to maximize sensitivity, as in the case of the very high-sensitivity Raman equipment of our institute.¹³⁻¹⁷

To make things concrete, let us take SF_6 and its $2\nu_5$ Raman overtone. This molecule has been witnessing re-

newed spectroscopic interest in the last two decades,¹⁸⁻²⁵ with its role in environmental and atmospheric issues being among the reasons for concern.²⁶⁻²⁸ At room temperature, the overtone $2\nu_5$ manifests itself as a highly polarized weak-intensity spectrum,^{29,30} which is almost completely drowned out in a plethora of hot or difference band transitions that all are simultaneously "excited" at nearly the same frequency ($\sim 1048 \text{ cm}^{-1}$). Whereas in all those transitions the vibrational quantum number associated with ν_5 makes a jump from $\nu_5 = 0$ to $\nu_5 = 2$, one or several ν_i ($i \neq 5$) modes of the molecule may have remained excited in an arbitrary vibrational level ν_i during the transition. Matrix elements such as $\langle 000021|\alpha|000001\rangle$, $\langle 000022|\alpha|000002\rangle$, $\langle 000120|\alpha|000100\rangle$ are typical of such a type of bands, taken arbitrarily from the pool of transitions around the frequency value 1048 cm^{-1} . These are identified as the hot bands $\nu_6 + 2\nu_5 - \nu_6$, $2\nu_6 + 2\nu_5 - 2\nu_6$, and $\nu_4 + 2\nu_5 - \nu_4$, respectively, and in a way analogous to many others, they can greatly affect the spectrum of the "pure $2\nu_5$ overtone" and wrongly be thought of as pertaining to the transition $\langle 000020|\alpha|000000\rangle$. Worse, a multitude of other hot bands also occurs at nearly the same frequency, owing to an initially excited vibrational level ν_5 . Among the large number of such bands, one may quote the $3\nu_5 - \nu_5$, the $4\nu_5 - 2\nu_5$, or even combinations of the type $\nu_6 + 3\nu_5 - (\nu_6 + \nu_5)$ or $2\nu_6 + 3\nu_5 - (2\nu_6 + \nu_5)$, with matrix elements $\langle 000030|\alpha|000010\rangle$, $\langle 000040|\alpha|000020\rangle$, $\langle 000031|\alpha|000011\rangle$, and $\langle 000032|\alpha|000012\rangle$, respectively. The question then arises: Is it possible to isolate from the experimentally measured integrated cross-section the bare overtone contribution $\langle 000020|\alpha|000000\rangle$? In many systems, there is a reduced number of hot bands in the vicinity of a transition, so what in fact one measures, there, is to a good

^{a)}Electronic mail: michel.chrysos@univ-angers.fr

approximation the real transition alone. In those cases there is not even a question to answer. But in the case of SF₆ (especially for low-frequency bending modes) things can be very different. This is even more so upon treating hot gas. Not only the severe coalescence that occurs at high gas pressure or temperature conditions makes it impossible to isolate (000020|α|000000), but even if it were possible to do so it would be of limited interest, resulting in matrix elements that are temperature-dependent. What in fact matters in making such an experiment is to extract information inherent in the molecule, namely, some value for the physically relevant effective second polarizability derivative $(\partial^2\alpha/\partial q_i^2)_{\text{eff}}$ (Ref. 31). This derivative is, by construction, the same for all the matrix elements pertaining to the spectrum, which will only differ in proportionality factors that can be worked out analytically.

It is the purpose of this paper to report on the link between the integrated overtone spectrum M_0 and the harmonic property $(\partial^2\alpha/\partial q_i^2)$. In the harmonic approximation these formulas are exact. In the presence of anharmonicity, $(\partial^2\alpha/\partial q_i^2)_{\text{eff}}$ should instead be viewed as the anharmonic derivative in the (000020|α|000000) transition, which differs from $(\partial^2\alpha/\partial q_i^2)$ in (v -independent) anharmonic corrections. In certain situations, such as for modes v_i and conditions ensuring $\frac{h\nu_i}{k_B T} \ll 1$, weakly coupled vibrations and small cubic force constants k_{kii} ($k \neq i$), as in the case treated in the example to be developed below, the harmonic approximation is enough. Yet, even in the most unfavorable cases, the content of this paper will be of value for assessing the otherwise unsuspected degree of difficulty in treating a multiply degenerated low-energy bending mode of a high-symmetry molecule, which by nature is closer to an infinitely degenerated gas than to an ordinary few-levels textbook system.

II. THEORY

A. Past and current trends

There is long evidence that absorption or scattering cross-sections can increase with temperature. Reports have appeared in the 1960s claiming an increase by a factor 1000 in the mean polarizability of molecular hydrogen upon heating the gas to 5000 K and averaging the vibrational³² and rotational^{33,34} states. Surprising effects such as the “cold-band effect” were seen experimentally, in the early 1980s, in which the $3\nu_3$ absorption cross-section of SF₆ was found to decrease with increasing temperature.³⁵ A few years later, absorption experiments with SF₆ showed the existence of enhanced hot-band multiphoton absorption.³⁶ The use of cryostatic cells and jet-cooled equipment to reduce the effect of hot bands also goes back to that time^{37,38} and still continues nowadays.^{39,40} Late in the 1980s, refraction index experiments, carried out by Hohm and Kerl, have shown how to monitor the temperature dependence of electronic polarizability for molecular and atomic gases.^{41,42} As for theory, internal-coordinate formulations for the vibration-rotation energies of octahedral spherical top molecules have allowed to determine partial sets of cubic potential energy coefficients in the normal and symmetry coordinate bases.⁴³ Similar sets of data were almost

simultaneously reported by other scientists, on the basis of experiments or calculations for SF₆ (Refs. 44 and 45). More recently, new techniques for constructing representations of point groups, that are particularly useful when describing high overtones, have been introduced.⁴⁶

In what follows, we focus on sulfur hexafluoride and on its vibrational spectra and derivatives, which are timely issues to deal with.^{27,28} Of the six vibration modes of SF₆, only ν_3 and ν_4 are IR active, and thus directly involved in radiative forcing. Pure bending modes, such as the scissoring vibration ν_5 on which our paper mainly focuses, do not directly involve deformation of the S–F bond. This fact explains the origin of the believed small or even tiny value of the anharmonicity constant k_{155} [$= \frac{\phi_{155}}{2} = C_{155} = -17 \text{ cm}^{-1}$ (Ref. 44), 0.68 cm^{-1} (Ref. 45)] and of the difficulty in obtaining reliable data for that quantity.⁴⁷ In this respect, Krohn and Overend have come to the conclusion that their “*calculated values of C_{155} and C_{166} may not be reliable*” and that “*incompleteness in the bending and stretch-bend anharmonicities is responsible for shortcomings in calculations involving the lower-frequency modes.*”⁴⁴ Similar are the conclusions of Hodgkinson, Barrett, and Robiette,⁴⁵ who have pointed out that cubic constants which only involve the interactions of stretching vibrations are an order of magnitude larger than those involving the bending vibration ν_5 , and that their “*general model is not particularly accurate for stretch-bend constants.*” Although the need for improved spectroscopic data and for explicit account of stretch-bend and bend-bend interactions in the force field of SF₆ appears clearly already in the mid-1980s (Ref. 45, p. 945), 25 years later there is still no improvement in this area. This need is timelier today than ever before in view of the recent conclusions of NASA scientists: the bond derivatives (especially the ones involving fluorine atoms) have been identified as being responsible for the molecular origin of greenhouse warming.⁴⁸

B. Vibrational partition functions and populations

To represent the states over which the vibrational energy, $E_{\vec{v}}$, of the gas molecules is distributed in thermodynamic equilibrium, m -uplets $\vec{v} = (v_1, v_2, \dots, v_m)$ pertaining to the ensemble \mathbb{N}^m are used, where m is the number of molecular normal modes and v_i are the associated vibrational quantum numbers. For SF₆, $m = 6$. According to Boltzmann statistics, the fraction of SF₆ molecules occupying a sixuplet \vec{v} , at temperature T , reads:

$$P_{\vec{v}} = \frac{1}{Z} \prod_{i=1}^m g_{n_i,i}(v_i) e^{-v_i x_i}, \quad (1)$$

where $x_i = \frac{h\nu_i}{k_B T}$ and

$$Z = \sum_{v_i=0}^{\infty} \prod_{i=1}^m g_{n_i,i}(v_i) e^{-v_i x_i} \quad (2)$$

is the total vibrational partition function in which the contribution of the zero-point vibrational energy has been removed (more about this intentional omission is said below). In the above formulas, ν_i is the fundamental frequency of mode i ,

and n_i its degeneracy. $g_{n_i,i}(v_i)$ stands for the degeneracy of the v_i th excited state of this mode. The calculation of $g_{n_i,i}(v_i)$, for a molecule vibrating harmonically in an n_i -fold degenerated mode v_i , addresses notions of combinatorics to answer the question: “in how many different ways can one satisfy $a_1 + a_2 + \dots + a_{n_i} = v_i$, where a_1, a_2, \dots, a_{n_i} are non-negative integers?” In the case of $i = 1$, which, in both SF₆ and CO₂, is a totally symmetric vibration, ν_1 is a non-degenerated mode ($n_1 = 1$) and there is only one way to satisfy the aforementioned condition. As a result, $g_{n_1,1}(v_1) = 1$ whatever the value v_1 . In the case of ν_2 ($i = 2$), which for both those molecules is a doubly degenerated mode ($n_2 = 2$), there are obviously $g_{n_2,2}(v_2) = v_2 + 1$ ways to satisfy the condition $a_1 + a_2 = v_2$. Finally, in the case of the vibrations ν_3, ν_4, ν_5 , and ν_6 of SF₆ ($i = 3, \dots, 6$), which are all triply degenerated ($n_i = 3$), one can readily check that there are $g_{n_i,i}(v) = \frac{1}{2}(v_i + 1)(v_i + 2)$ ways to satisfy $a_1 + a_2 + a_3 = v_i$. The three specific formulas given above for $n_i = 1, 2$, and 3 can readily be generalized to any value of n_i through the formula:⁴⁹

$$g_{n_i,i}(v_i) = \frac{(v_i + n_i - 1)!}{(n_i - 1)!v_i!}. \quad (3)$$

Table I gathers, in the order of decreasing probability, the 33 sixuplets \vec{v} that were necessary for convergence to 95% of the fractional population of SF₆ at room temperature, along with degeneracy $g(\vec{v}) [= \prod_{i=1}^6 g_{n_i,i}(v_i)]$, vibrational energy $E_{\vec{v}}$ (in cm⁻¹), and occupation probability $P_{\vec{v}}$ for the state \vec{v} at that temperature. At 295 K, only 32% of the molecules are in the ground vibrational state. The next three excited states, (000001), (000010), and (000002), contain together as many molecules as the ground state itself. The missing 5% of the population is spread over a huge number of states (not shown). More than 15% of the total population is distributed over levels that are only very little occupied (<1%). Similar data, but limited to the 15 most populated states, have been reported in the past;⁵⁰ wherever the comparison is possible, excellent agreement between the two series of data is found.

Rearrangement between the product and the sum operators in the expression of Eq. (2) allows one, with the help of Eq. (3), to deduce the very useful formula:⁵¹

$$Z = \prod_{i=1}^m (Z_i)^{n_i}, \quad (4)$$

where $Z_i = (1 - e^{-x_i})^{-1}$ is the vibrational partition function for a single degree of freedom of vibration i . As mentioned above, the zero-point vibrational energy is missing in the expression $Z_i = (1 - e^{-x_i})^{-1}$, which should instead read: $Z_i = e^{-\frac{x_i}{2}}(1 - e^{-x_i})^{-1}$. Yet there are good reasons why we might want to remove this factor from the definition of Z_i (Ref. 52).

Application of Eq. (4) to the case of SF₆ results in the very useful and simple expression:

$$Z = (1 - e^{-x_1})^{-1}(1 - e^{-x_2})^{-2} \times [(1 - e^{-x_3})(1 - e^{-x_4})(1 - e^{-x_5})(1 - e^{-x_6})]^{-3}. \quad (5)$$

TABLE I. States of SF₆ sharing, at 295 K, 95% of the total gas population. The states are sorted in the order of decreasing probability. States occupied to <1% share 15% of the total fractional population. The vector \vec{v} denotes the sixuplet ($v_1 v_2 v_3 v_4 v_5 v_6$).

\vec{v}	$g(\vec{v})$	E (cm ⁻¹)	$P_{\vec{v}}$ (%)
(000000)	1	0	31.839
(000001)	3	348.08	17.490
(000010)	3	523.56	7.432
(000002)	6	696.16	6.405
(000100)	3	615.02	4.758
(000011)	9	871.64	4.083
(010000)	2	643.35	2.762
(000101)	9	963.10	2.614
(000003)	10	1044.24	1.955
(010001)	6	991.43	1.518
(000012)	18	1219.72	1.495
(000020)	6	1047.12	1.157
(000110)	9	1138.58	1.111
(000102)	18	1311.18	0.957
(001000)	3	947.98	0.938
(100000)	1	774.55	0.728
(010010)	6	1166.91	0.645
(000021)	18	1395.20	0.635
(000111)	27	1486.66	0.610
(010002)	12	1339.51	0.556
(000004)	15	1392.32	0.537
(001001)	9	1296.06	0.515
(000200)	6	1230.04	0.474
(000013)	30	1567.80	0.456
(010100)	6	1258.37	0.413
(100001)	3	1122.63	0.400
(010011)	18	1514.99	0.354
(000103)	30	1659.26	0.292
(000201)	18	1578.12	0.260
(000022)	36	1743.28	0.233
(010101)	18	1606.45	0.227
(000112)	54	1834.74	0.223
(001010)	9	1471.54	0.219

Table II gathers the values of the various partition functions of SF₆ at room temperature. The values of the entries suggest that ν_1 is, thermodynamically, the least active mode, for it is both non-degenerated and energetic. The opposite holds true for modes ν_6 and ν_5 , and to a lesser extent for mode ν_4 , for they are all triply degenerated and of lower energy.

TABLE II. Partition functions of the different normal vibration modes. n_i stands for the oscillator dimension. The total vibrational partition function amounts to $Z = 3.141$ at $T = 295$ K. v_i are given in cm⁻¹. The calculation of Z_i 's was done analytically.

Mode	$i = 1$	$i = 2$	$i = 3$	$i = 4$	$i = 5$	$i = 6$
v_i	774.55	643.35	947.98	615.02	523.56	348.08
n_i	1	2	3	3	3	3
$g_{n_i,i}(v_i)$	1	$v_i + 1$		$\frac{1}{2}(v_i + 1)(v_i + 2)$		
$(Z_i)^{n_i}$	1.023	1.093	1.030	1.166	1.275	1.835

C. Raman cross-sections and hot bands

1. First overtones of triply degenerated vibrations

In the case of a threefold degenerated mode ν_i , the initial state of the molecule is designated by a triplet $(v_{i,1}, v_{i,2}, v_{i,3})$ of quantum numbers $v_{i,1}$, $v_{i,2}$, and $v_{i,3}$, which obey $v_i = v_{i,1} + v_{i,2} + v_{i,3}$ and are associated with three equivalent, independent degrees of freedom. As a result, there are six possible final states involved in the upward overtone transition $v_i \rightarrow v_i + 2$, which read: $(v_{i,1} + 2, v_{i,2}, v_{i,3})$, $(v_{i,1}, v_{i,2} + 2, v_{i,3})$, $(v_{i,1}, v_{i,2}, v_{i,3} + 2)$, $(v_{i,1} + 1, v_{i,2} + 1, v_{i,3})$, $(v_{i,1} + 1, v_{i,2}, v_{i,3} + 1)$, $(v_{i,1}, v_{i,2} + 1, v_{i,3} + 1)$. For the first three, the corresponding matrix-elements of the dipole-dipole polarizability tensor invariant α read:

$$\frac{\sqrt{(v_{i,p} + 1)(v_{i,p} + 2)}}{2} \left(\frac{1}{2!} \frac{\partial^2 \alpha}{\partial q_{i,p}^2} \right),$$

where $p = 1, 2, 3$. For the remaining three final states, the matrix-elements are

$$\frac{\sqrt{(v_{i,p} + 1)(v_{i,q} + 1)}}{2} \left(\frac{1}{2!} \frac{\partial^2 \alpha}{\partial q_{i,p} \partial q_{i,q}} + \frac{1}{2!} \frac{\partial^2 \alpha}{\partial q_{i,q} \partial q_{i,p}} \right),$$

with $p, q = 1, 2, 3$ and $p < q$. The derivatives are calculated at the equilibrium position.

Given that the scattering process is incoherent, the interference terms make no net contribution to the intensity, and the Raman zeroth-order moment is simply the sum of the probability averages. Use of symmetry properties further simplifies the calculation of the moment, which reads:

$$M_0 = \frac{3}{16} \left(\frac{\partial^2 \alpha}{\partial q_{i,1}^2} \right)^2 \frac{\sum_{v=0}^{\infty} e^{-v x_i} (v+1)(v+2)}{\sum_{v=0}^{\infty} e^{-v x_i}} + \frac{3}{4} \left(\frac{\partial^2 \alpha}{\partial q_{i,1} \partial q_{i,2}} \right)^2 \left(\frac{\sum_{v=0}^{\infty} e^{-v x_i} (v+1)}{\sum_{v=0}^{\infty} e^{-v x_i}} \right)^2.$$

Repeating use ($k = 0, 1, 2$) of the very useful formula

$$\sum_{v=0}^{\infty} v^k e^{-v x_i} = \left(-\frac{d}{dx_i} \right)^k (1 - e^{-x_i})^{-1} \quad (6)$$

allows us to calculate the two sum-ratio terms in the rhs of the above equation, which acquire the simple expressions $2(1 - e^{-x_i})^{-2}$ and $(1 - e^{-x_i})^{-2}$, respectively. Thus M_0 reads:

$$M_0(T) = \frac{3}{8} \gamma_i(T) \left[\left(\frac{\partial^2 \alpha}{\partial q_{i,1}^2} \right)^2 + 2 \left(\frac{\partial^2 \alpha}{\partial q_{i,1} \partial q_{i,2}} \right)^2 \right], \quad (7)$$

with

$$\gamma_i(T) = \left(1 - e^{-\frac{h\nu_i}{k_B T}} \right)^{-2}. \quad (8)$$

The quantity $\gamma_i(T)$, hereinafter referred to also as the γ -factor, has the meaning of a ‘‘hotband factor,’’ for it describes the scattering cross-section of the overtone at the temperature of the experiment normalized to the cross-section of the same overtone at 0 K.

It was gratifying to find out that the expression of Eq. (7) leads directly to the cross-section for the \perp component $d\sigma_{\perp}/d\Omega$ long ago reported in the analysis of the $2\nu_4$ overtone of cyanogen.⁵³ For the latter analysis, a technically exhaustive lengthy mathematical approach had been applied, involving symmetry-adapted normal coordinates and spherical-oscillator algebra mostly addressed to theorists.

2. The $2\nu_5$ overtone

There is sparse evidence of Raman overtones from greenhouse molecules, and only recently has their treatment (CO_2 , $2\nu_3$) begun to be completed.^{54–57} No calibrated spectrum and far too synoptic material on the Raman $2\nu_5$ overtone of SF_6 was found in the so far existing literature, even though evidence for a strongly polarized band has twice been reported.^{29,30} In spite of the very low resolution [6 cm^{-1} (Ref. 29), $3\text{--}10 \text{ cm}^{-1}$ (Ref. 30)] that these scientists have employed in their experiments (far lower than our 0.85 cm^{-1}), no or little mention of the role of the hot bands has been made, while the fact of keeping fixed the incident-beam polarization (perpendicular to the scattering plane) further hindered them from reporting on the isotropic spectrum of the overtone.

Given the strongly polarized character of that band, the Raman spectrum of $2\nu_5$ should merely be isotropic and only derivatives of the mean-polarizability invariant, $\bar{\alpha}$, will be involved in the analysis. Further simplification comes from the observation that the contribution of the cross second derivatives of $\bar{\alpha}$ is zero. A simple argument to show this property is based on symmetry considerations and runs as follows: if we rotate the molecule around $q_{i,3}$ so that the coordinate $q_{i,1'}$ coincides with $q_{i,2}$ and the $q_{i,2'}$ switches to $-q_{i,1}$, the second cross derivative of the polarizability trace changes sign, a result only compatible with $\frac{\partial^2 \bar{\alpha}}{\partial q_{i,1} \partial q_{i,2}} = 0$ (endomorphism).

These properties lead to the following expression for the zeroth-order isotropic moment:

$$M_0 = \frac{3}{2} \left(1 - e^{-\frac{h\nu_i}{k_B T}} \right)^{-2} \left(\frac{1}{2} \frac{\partial^2 \bar{\alpha}}{\partial q_5^2} \right)_{\text{eff}}^2. \quad (9)$$

Here, the specification ‘‘eff’’ makes reference to the fact that the second derivative of Eq. (9) has accounted effectively for anharmonic corrections. The second index in $q_{5,1}$ was dropped for simplicity.

The expression of Eq. (9) is formally very different from what would be observed in the absence of hot bands: in their absence, it is the spectral moment $M_0^{2\leftarrow 0} = \lim_{T \rightarrow 0} M_0(T)$ of the bare overtone transition $(000020) \leftarrow (000000)$ that would have instead been measured. In the case of room-temperature SF_6 , one has $P_0 = 0.32$ (see Table I), a value far from being close to 1. As a result, only ideally can the quantity $M_0^{2\leftarrow 0}$ be isolated from its environment and be measured, especially upon raising gas pressure up to several atmospheres to make the tiny overtone signal be detectable. Interestingly, the low frequency of the ν_5 mode (see Table II) makes the values of $\gamma_i(T)$ to literally take off above $T \approx 300 \text{ K}$ and the intensity of the overtone to be doubled at $300 \text{ }^\circ\text{C}$ (see below).⁵⁸

TABLE III. Energy distribution of fractional SF₆ populations and contributions to the hotband γ -factor of the overtone. For the purpose of this table, these contributions were computed numerically in order to monitor their convergence to the value given by Eq. (8).

Energy (cm ⁻¹)	<1000	<2000	<3000	<4000
Number of states	15	157	852	3183
Fractional population (%)	80.71	97.88	99.86	99.99
Contribution to the γ -factor	0.884	1.137	1.172	1.175

3. Distribution of the scattered intensity over energy

According to our computations, at room temperature, 98% of the contributions to the gas population and to the hotband γ -factor of Eq. (8) are from vibrational states with energies lying below 2000 cm⁻¹ and $v_5 \leq 2$. This is inferred from the data of Tables III and IV. The first of these tables allows one to analyze these contributions as a function of the width of the energy window and of the number of vibrational states considered in the computation. The second table displays how the population of the gas molecules and their contributions to the $2\nu_5$ Raman signal are shared on the v_5 ladder.

Figure 1 illustrates the way in which the molecular population of SF₆ (boxes) and its contribution to the γ -factor of Eq. (8) (lines) are distributed for the $2\nu_5$ overtone, as a function of vibrational energy at room temperature. On climbing the energy ladder, the convergence to the result of Eq. (8) for $2\nu_5$ is enough fast to make mechanical anharmonicity not to have a significant effect at room temperature. This convergence is considered effective as soon as the energy has reached 2100 cm⁻¹.

Figures 2 and 3 show how molecular population of SF₆ (dark grey sticks) along with contributions to the hotband γ -factor of Eq. (8) (light grey sticks) are distributed as a function of $v_{tot} (= \sum_{i=1}^6 v_i)$ and v_5 , respectively. As seen from these figures, in order for the convergence to the $\gamma_i(295\text{K})$ value to be almost complete, it suffices to climb the v -steps up to $v_{tot} = 5$ and $v_5 = 2$. This finding suggests that the anharmonicity of the SF₆ potential should have only a reduced effect in the treatment of $2\nu_5$ at room temperature.

Figure 4 illustrates the behavior of the hotband factor of Eq. (8) as a function of temperature (in K), for three representative $2\nu_i$ overtones of SF₆ (solid line curves). These are in the descending order: $2\nu_6$ (black solid line), $2\nu_5$ (blue solid line), $2\nu_1$ (red solid line). Note that the most significant variations are due to the low energy of the corresponding modes

TABLE IV. Fractional populations of SF₆ molecules and their contributions to the Raman intensity of the overtone for different values of the initial state vibrational number v_5 at 295 K. All contributions due to other modes have already been accounted for in the calculation of the entry values.

v_5	$P(v_5)$ (%)	Scattered intensity (%)
0	78.56	66.88
1	18.22	25.85
2	2.82	6.00
3	0.36	1.08
4	0.04	0.17
5	0.00	0.02

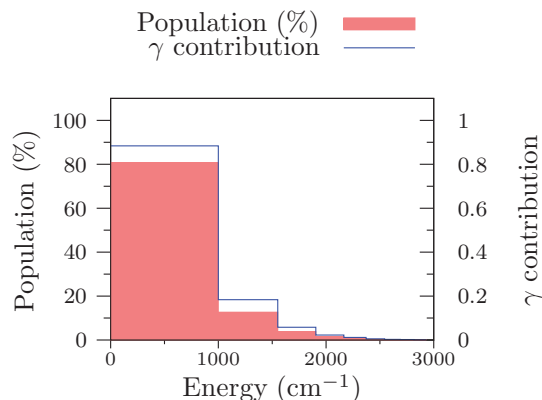


FIG. 1. Fractional population of gas molecules (boxes) and contributions to the overtone γ -factor of Eq. (8) (lines) as a function of vibrational energy range (in units of cm⁻¹) at 295 K.

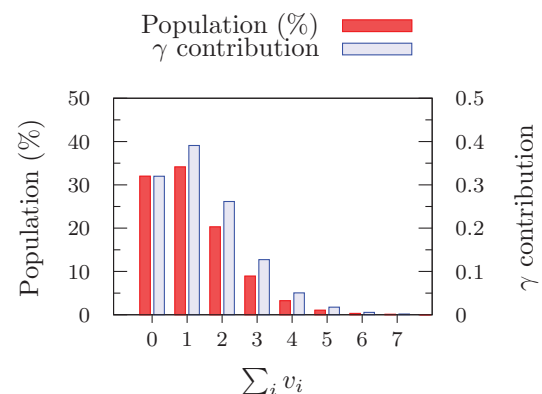


FIG. 2. Fractional population of gas molecules (dark grey sticks) and contributions to the overtone γ -factor of Eq. (8) (light grey sticks) as a function of $v_{tot} = \sum_i v_i$ at 295 K.

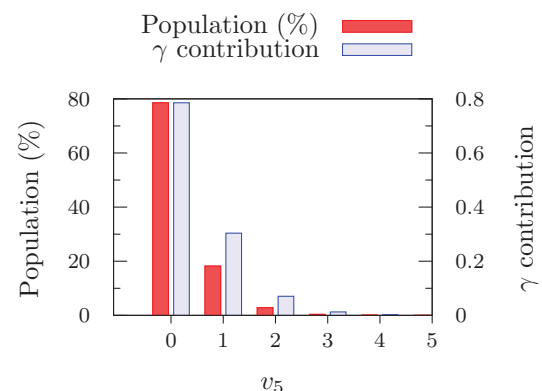


FIG. 3. Fractional population of gas molecules (dark grey sticks) and contributions to the overtone γ -factor of Eq. (8) (light grey sticks) as a function of v_5 at 295 K.

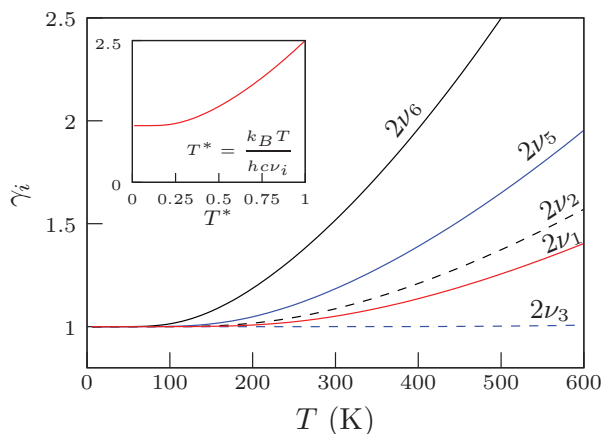


FIG. 4. Temperature dependence of the γ -factor for three overtones of SF₆ (solid line curves). From top to bottom: $2\nu_6$ (black solid line), $2\nu_5$ (blue solid line), $2\nu_1$ (red solid line). For comparison, the factors of the $2\nu_2$ and $2\nu_3$ overtones of CO₂ have also been plotted (dashed line curves). In the inset, the γ -factor is shown as a function of reduced temperature $T^* = k_B T / (h c \nu_i)$.

(348 and 524 cm⁻¹ for ν_6 and ν_5 , respectively). The more energetic ν_1 mode (774 cm⁻¹) is by far less affected by temperature. For the sake of comparison, the factors that are relative to the $2\nu_3$ and $2\nu_2$ overtones of CO₂ are also shown (dashed line curves). To make it possible to compare, whatever the molecule, how the hotband factor depends simultaneously on T and ν_i , a reduced temperature $T^* = \frac{k_B T}{h c \nu_i}$ was introduced⁵⁹ and the plot of γ_i as a function of T^* is shown in the inset. The value $T^* = 1$ corresponds to a fictitious mode with energy equal to that of the thermal excitation; at room temperature, this mode is activated at 205 cm⁻¹. Below $T^* = 0.2$, the hotband factor makes almost no effect. At room temperature, this behavior would correspond to modes with frequencies greater than 1025 cm⁻¹. None of the SF₆ modes has such a high frequency. In contrast, the two stretching modes of CO₂ do belong to this class, and the impact of the thermal factor for CO₂ becomes tiny.

III. EXPERIMENT

The experiment was carried out using equipment well known for its sensitivity and a meticulous and stiff protocol that we have established to ensure reliability in the signal extraction. Description in detail of the equipment and of the way we are used to operate has been given previously.^{13, 14, 17, 60, 61} Technical details, related to the way in which the $2\nu_5$ signal was isolated from its environment and to how a density-independent absolute-calibrated isotropic spectrum was extracted from the recorded spectrum, will be skipped. In what follows, only the essentials of the isotropic spectrum are gathered.

A. Setup, settings, and detection

A solid-state 532-nm frequency-doubled Nd:YV04 laser was used to shine green light onto high purity (99.995%) pressurized sulfur hexafluoride gas. The sample was maintained at a constant temperature of 294.5 ± 1 K and confined in a four-

window cell specially designed to support high pressures. Raman signals scattered thereby at a right angle were recorded. A nitrogen-cooled CCD was used for the detection. The laser power was kept constant at 2 W for all the runs. Various gas densities covering the range from 2 to 27 amagat were used, that is, pressures going from ~ 2 to 20 atm.

The center of the $2\nu_5$ overtone was seen at 1048 cm⁻¹ and the band was recorded over a wide frequency interval, ν , ranging from 980 to 1150 cm⁻¹. At each experimental run and setting value for the gas density, calibration of the Raman signal (photons/second) was made to an absolute-scale density-dependent (amagat cm³) signal intensity $S(\nu)$ by means of the $S_0(1)$ rotational line of molecular hydrogen. This line was centered at 587.1 cm⁻¹. A switchable linear polarization for the incident beam was used, giving rise to independent Raman signals $S_{\parallel}(\nu)$ and $S_{\perp}(\nu)$. These signals were then combined together in a linear combination with appropriate coefficients⁵⁵ to form the isotropic signal $S_{iso}(\nu)$. To make sure that the recorded spectrum was indeed due to transitions by single SF₆ molecules, a rigorous protocol was applied, enabling us to determine the exact way in which the gas density, ρ , affects the integrated signal (S_{iso})_{int}. A behavior that is strictly linear in ρ was observed, which is compelling evidence that the isotropic spectrum was indeed due to isolated SF₆ molecules. The density-independent isotropic intensity profile was then deduced through $I_{iso}(\nu) = S_{iso}(\nu)/\rho$.

In Figure 5, the absolute-calibrated density-dependent spectra S_{iso} are illustrated on a semi logarithmic scale as a function of Raman frequency (in cm⁻¹), for the various gas densities employed and after extraction of the surrounding parasitic signals. The deleted stripe seen on the plot around the frequency 1034.7 cm⁻¹ corresponds to the position where the hydrogen rotational line $S_0(3)$ appeared and perturbed the SF₆ spectrum. This range was covered by interpolation before any integration of spectra. The straight line shown in the

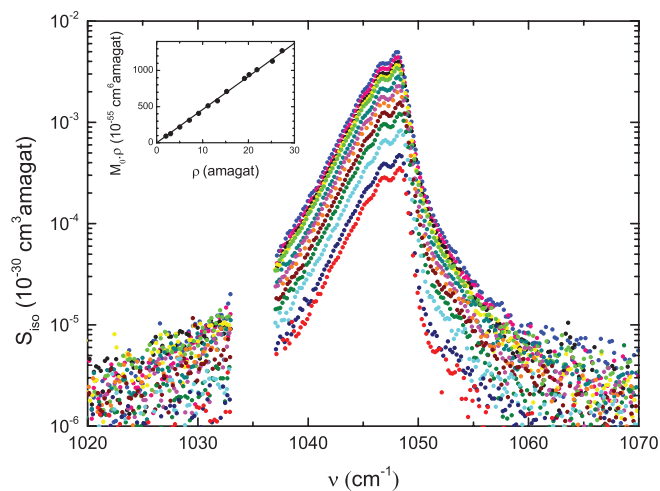


FIG. 5. Absolute-calibrated spectra S_{iso} (in units of cm³ amagat) as a function of Raman frequency ν (in units of cm⁻¹) for 13 values of gas density ranging from 2 to 27 amagat (in the upward direction). In the inset, the product $M_0 \cdot \rho$ [M_0 is the experimental zeroth-order moment (in units of cm⁶) of the signal generated from a gas sample of density ρ] is shown as a function of ρ (in units of amagat). The linear dependence is evidence that the recorded band comes from isolated molecules alone.

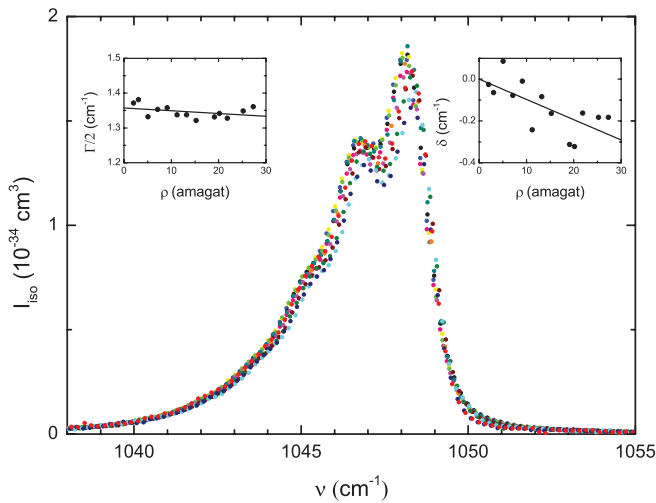


FIG. 6. Isotropic spectrum I_{iso} (in units of cm^{-3}) as a function of Raman frequency ν (in units of cm^{-1}) for 13 values of gas density ranging from 2 to 27 amagat (in the upward direction; same colors as in Fig. 5). The small differences between the spectra (especially at the top) is an indication of weak but distinguishable pressure-induced effects modifying the shape of the overtone. In the insets the half-width $\Gamma/2$ at $1/\sqrt{e}$ -maximum and the band-top shift δ (in units of cm^{-1}) are shown as a function of density ρ (in units of amagat).

inset represents the quantity $M_0\rho$ as a function of ρ , with M_0 the zeroth-order isotropic moment. Given the definition of M_0 [see below Eq. (10)], the perfect alignment of the points in the inset is evidence for spectrum integrals $\int_{-\infty}^{\infty} S_{iso}(\rho, \nu) d\nu$ scaling linearly with ρ .

Figure 6 shows the isotropic spectrum, I_{iso} , as a function of ν , for the different values of ρ . The close resemblance of the spectra is indication of small yet observable pressure-induced effects for this overtone. The precise way in which broadening and shift were found to depend on ρ is shown in the insets: A tiny negative broadening (narrowing), scaling linearly with ρ and amounting to $-8 \times 10^{-4} \text{ cm}^{-1}/\text{amagat}$ is seen along with a redshift about ten times greater. The small dispersion of points, both in the main body of the figure and in the insets, is a measure of the quality of our measurements.

B. Accounting for the surrounding bands

A major difficulty in the study of the overtone came from the far wing of certain transitions such as the very intense fundamental ν_1 (centered at 774 cm^{-1}) or the collision-induced component of ν_3 (centered at 948 cm^{-1}), which severely perturbed the baseline of the $2\nu_5$ signal. Another perturbation occurred due to the presence of undesired signals located at the upper frequency side of the $2\nu_5$ overtone, which were interpreted as being possibly due to the far wings of the $\nu_2 + \nu_5$ combination band and to a lesser extent due to the $2\nu_4$ and $2\nu_2$ overtones, centered at 1166 , 1230 , and 1285 cm^{-1} , respectively. The perturbation of the latter three signals, although substantial, was less significant than that of the lower frequency signal. For all of them, a systematic least-squares fitting procedure was applied employing an exponential wing profile (adapted to the perfectly linear aspect seen on a logarithmic plot for the spectral tails) and 13 experimental runs for

TABLE V. Scattering cross-sections for the overtone by using incident light polarized \perp to the scattering plane.

$\frac{d\sigma_{\perp}}{d\Omega} (\times 10^{-33} \text{ cm}^2 \text{ sr}^{-1})$	
This work	0.96
Previous works	0.93 ^a
	0.61 ^b

^aReference 30.

^bReference 29.

gas densities covering the range from 2.03 to 27.34 amagat. Thorough analysis of that careful procedure will be reported elsewhere. The spectra of Figures 5 and 6 were obtained after extraction of the surrounding parasitic signals.

C. The spectral moment

The isotropic zeroth-order moment was calculated by integrating the isotropic spectral intensity $I_{iso}(= \frac{S_{iso}}{\rho})$, by means of the formula:

$$M_0 = [2\pi(\nu_0 - \nu_s)]^{-4} \int_{-\infty}^{+\infty} I_{iso}(\nu) d\nu. \quad (10)$$

In the latter expression, ν_0 denotes the laser wavenumber and ν_s the wavenumber at the center of the recorded band. The result is in units of cm^6 . We obtained the value $M_0(\text{expt.}) = 4.59(69) \times 10^{-54} \text{ cm}^6$.

Table V gathers previous and present results for scattering cross-sections obtained with incident beam polarization perpendicular to the scattering plane.

IV. CALCULATIONS

A. Derivatives

Given the value of M_0 extracted from the recorded isotropic spectrum, we are now able to deduce, on the basis of Eq. (9), the value $|(\partial^2 \bar{\alpha} / \partial q_5^2)_{\text{eff}}| = 0.0218 a_0^3$ (a_0 is the Bohr radius). Further refinement of the analysis is possible upon using anharmonicity data that are either available or that are yet to come. Thus, by assuming that the anharmonicity corrections are independent of the vibration quantum number (which is a reasonable assumption for enough low-lying vibrational excitations ν_5 and ν_{10i} ; see Table IV, Figures 2 and 3), the harmonic derivative $\partial^2 \bar{\alpha} / \partial q_5^2$ reads:

$$\frac{\partial^2 \bar{\alpha}}{\partial q_5^2} = \left(\frac{\partial^2 \bar{\alpha}}{\partial q_5^2} \right)_{\text{eff}} - \frac{\partial \bar{\alpha}}{\partial q_1} k_{155} \frac{2\nu_1}{4\nu_5^2 - \nu_1^2}. \quad (11)$$

This expression stems from the most general expression⁶² relevant to overtone transition matrix-elements $\langle \dots \nu_i + 2 \dots | \bar{\alpha} | \dots \nu_i \dots \rangle$:

$$\left(\frac{\partial^2 \bar{\alpha}}{\partial q_i^2} \right)_{\text{eff}} = \frac{\partial^2 \bar{\alpha}}{\partial q_i^2} + \frac{\partial \bar{\alpha}}{\partial q_i} \frac{2k_{iii}}{\nu_i} + \sum_{k \neq i} \left[\frac{\partial \bar{\alpha}}{\partial q_k} k_{kii} \frac{2\nu_k}{4\nu_i^2 - \nu_k^2} \right] \quad (12)$$

upon setting $i = 5$, $k = 1$, and $\partial \bar{\alpha} / \partial q_i = 0$. The latter condition is a consequence of the fact that ν_5 is a vibration that is

TABLE VI. Values for $(\partial^2\bar{\alpha}/\partial q_i^2)_{\text{eff}}$ and $(\partial^2\bar{\alpha}/\partial q_i^2)$ in units of a_0^3 .

$(\frac{\partial^2\bar{\alpha}}{\partial q_5^2})_{\text{eff}}$	$0.020^{\text{a,b}}$	$0.020^{\text{a,c}}$	$0.074^{\text{b,d}}$	$0.072^{\text{c,d}}$
0.0218	$0.020^{\text{a,b}}$	$0.020^{\text{a,c}}$	$0.074^{\text{b,d}}$	$0.072^{\text{c,d}}$
-0.0218	$-0.024^{\text{a,b}}$	$-0.024^{\text{a,c}}$	$0.030^{\text{b,d}}$	$0.028^{\text{c,d}}$

^aThe value $k_{155} = 0.68 \text{ cm}^{-1}$ was used (taken from Ref. 45).

^bThe value $\partial\bar{\alpha}/\partial q_1 = 0.975 a_0^3$ was used (taken from Ref. 63, expt.).

^cThe value $\partial\bar{\alpha}/\partial q_1 = 0.937 a_0^3$ was used (taken from Ref. 19, calculations).

^dThe value $k_{155} = -17 \text{ cm}^{-1}$ was used (taken from Ref. 44).

not totally symmetric and, as such, its fundamental transition gives rise merely to a depolarized spectrum. So too is the case with all the other derivatives $\partial\bar{\alpha}/\partial q_k$ in the summation over k , except for $k = 1$: of the six vibrations of SF₆, ν_1 is the only one to be totally symmetric (A_1).

The sign uncertainty in the value of the first rhs term in the above equation along with the very different magnitudes that have been reported for the cubic force constant k_{155} (Refs. 44 and 45) gives rise to a multitude of values for $\partial^2\bar{\alpha}/\partial q_5^2$. All of them were compatible with our spectrum. They are gathered in Table VI. The value of $\partial\bar{\alpha}/\partial q_1$ is known to a good accuracy both experimentally⁶³ and numerically (on the basis of second-order Møller-Plesset perturbation theory)¹⁹ but given the poor accuracy of k_{155} , the $\partial^2\bar{\alpha}/\partial q_5^2$ values are given to three decimal places.

Table VII gathers all the input data that were needed to apply Eq. (11). Polarizability derivatives are given in a_0^3 ; vibrational frequencies for the two modes and their cubic force constant are in cm^{-1} .

B. Higher order overtones

Before closing this section, it is worth noting that Eq. (9) is restricted to first overtones. It was almost effortless to extend it further to make it include overtones of any order, such as second overtones ($\Delta v_i = 3$) which are IR-allowed and known for their challenging spectra. A remarkably elegant formula is then obtained for the γ -factor along with a closed-form expression for the integrated isotropic spectral moment in the case of overtone bands “ $(\Delta v_i)\nu_i$ ” of arbitrary order for a non-degenerated vibration:

$$\gamma_i^{(\Delta v_i)} = \left(1 - e^{-\frac{h\nu_i}{k_B T}}\right)^{-\Delta v_i}, \quad (13)$$

$$M_0 = \frac{1}{2^{\Delta v_i} (\Delta v_i)!} \gamma_i^{(\Delta v_i)} \left(\frac{\partial^{\Delta v_i} \bar{\alpha}}{\partial q_{i,x}^{\Delta v_i}}\right)^2.$$

TABLE VII. Input data needed in Eq. (11). Polarizability derivatives are in a_0^3 units; vibrational frequencies and force constants are in cm^{-1} .

ν_1	ν_5	$\frac{\partial\bar{\alpha}}{\partial q_1}$	k_{155}
774.55	523.56	0.975 ^a	0.68 ^b
		0.937 ^c	-17 ^d

^aExpt.: Ref. 63.

^bAb initio calculations: Ref. 45.

^cAb initio calculations: Ref. 19.

^dAb initio calculations: Ref. 44.

Particular interesting is the fact that the hotband effect is greatly enhanced with increasing overtone order. For certain vibrations, the intensity of the $3\nu_i$ band can even be doubled at room temperature.

Note that, in spite of the diverging behavior $\lim_{h \rightarrow 0} \gamma_i^{(\Delta v_i)} = \infty$, the moments given above remain finite at the classical limit ($h \rightarrow 0$):

$$M_0^{\text{class}} = \frac{1}{2^{\Delta v_i} (\Delta v_i)!} \left(\frac{k_B T}{\mu_i (2\pi c \nu_i)^2}\right)^{\Delta v_i} \left(\frac{\partial^{\Delta v_i} \bar{\alpha}}{\partial r_{i,x}^{\Delta v_i}}\right)^2, \quad (14)$$

$r_i [= \sqrt{\hbar/(2\pi c \nu_i \mu_i)} q_i]$ and μ_i being the physical length coordinate and the reduced mass⁶⁴ associated with q_i , respectively, and $\partial^{\Delta v_i} \bar{\alpha}/\partial r_{i,x}^{\Delta v_i}$ the corresponding Δv_i -order derivative. Equation (14) shows that integrated intensities go with ν_i as $(T/\nu_i^2)^{\Delta v_i}$. Interestingly enough, changes in ν_i have a more pronounced effect on integrated spectra than they have it on bare γ -factors [$\gamma_i^{(\Delta v_i)} \sim (T/\nu_i)^{\Delta v_i}$, see Figure 4 for $\Delta v_i = 2$].

V. SYNOPSIS

Highly accurate absolute-calibrated Raman spectra were recorded from room-temperature pressurized SF₆ around the frequency of the highly polarized first overtone of the scissoring vibration ν_5 (1048 cm^{-1}). Experiments with 13 gas densities, ρ , ranging between 2 and 27 amagat were run. The profiles were seen to be only little affected by pressure and to obey rigorously a linear law in ρ . A systematic protocol was applied to remove effects due to the spectral wings of the accidentally present surrounding Raman bands, allowing us to rigorously determine the isotropic overtone spectrum. Full account was made of the multitude of hot bands around 1048 cm^{-1} , and a formula for $\partial^2\bar{\alpha}/\partial q_5^2$ was worked out involving a T -independent integrated intensity $M_0(T)/\gamma(T)$. Also, the issue of the much challenging IR-allowed second overtones was addressed in this article, through generalization of our formulas to elegant expressions that are applicable to overtones of any order for non-degenerated modes. In view of the growing attention that the issues of radiative forcing are being receiving internationally and of the fast 8% annual increase of SF₆ gas in the air, there is urgent need for *ab initio* calculated values of dipole moment and polarizability second derivatives like $\partial^2\bar{\alpha}/\partial q_5^2$. Not much seems to have emerged in that field since Maroulis’s contributions.¹⁹ Not only a fuller comparison between theory and experiment will in such a way be possible, also a reliable value for the thus-far loosely determined cubic force constant k_{155} will at last become available.

ACKNOWLEDGMENTS

One of us (D.K.) gratefully acknowledges doctoral fellowship support from the CNRS and “la Région des Pays de la Loire.”

¹G. C. Tabisz, in *Molecular Spectroscopy (a Specialist Periodical Report)*, edited by R. F. Barrow, D. A. Long and J. Sheridan, (Chemical Society, London, 1979), Vol. 6, pp. 136–173.

²E. Bright Wilson Jr., J. C. Decius, and Paul C. Cross, *Molecular Vibrations: The Theory of Infrared and Raman Vibrational Spectra* (Dover, New York, 1980).

- ³D. A. Long, *The Raman Effect: A Unified Treatment of the Theory of Raman Scattering by Molecules* (Wiley, Chichester, UK, 2002).
- ⁴L. Frommhold, *Adv. Chem. Phys.* **46**, 1 (1981).
- ⁵*Collision- and Interaction-Induced Spectroscopy*, edited by G. C. Tabisz and M. N. Neuman (Kluwer, Dordrecht, 1995).
- ⁶T. Bancewicz, Y. Le Duff, and J.-L. Godet, *Adv. Chem. Phys.* **119**, 267 (2001).
- ⁷L. Frommhold, *Collision-Induced Absorption in Gases* (Cambridge University Press, New York, 2006).
- ⁸J.-M. Hartmann, C. Boulet, and D. Robert, *Collisional Effects on Molecular Spectra: Laboratory Experiments and Model, Consequences for Applications* (Elsevier, Amsterdam, 2008).
- ⁹G. Avila, G. Tejada, J. M. Fernandez, S. Montero, *J. Mol. Spectrosc.* **220**, 259 (2003).
- ¹⁰J.-M. Hartmann, J.-P. Bouanich, K. W. Jucks, Gh. Blanquet, J. Walrand, D. Bermejo, J.-L. Domenech, and N. Lacome, *J. Chem. Phys.* **110**, 1959 (1999).
- ¹¹V. Boudon and N. Lacome, *J. Mol. Spectrosc.* **222**, 291 (2003).
- ¹²V. Boudon, J. L. Domenech, D. Bermejo, and H. Willner, *J. Mol. Spectrosc.* **228**, 392 (2004).
- ¹³F. Rachet, M. Chrysos, C. Guillot-Noël, and Y. Le Duff, *Phys. Rev. Lett.* **84**, 2120 (2000).
- ¹⁴F. Rachet, Y. Le Duff, C. Guillot-Noël, and M. Chrysos, *Phys. Rev. A* **61**, 062501 (2000).
- ¹⁵Y. Le Duff, *Phys. Rev. Lett.* **90**, 193001 (2003).
- ¹⁶M. Chrysos, A. P. Kouzov, N. I. Egorova, and F. Rachet, *Phys. Rev. Lett.* **100**, 133007 (2008).
- ¹⁷S. Dixneuf, M. Chrysos, and F. Rachet, *J. Chem. Phys.* **131**, 074304 (2009).
- ¹⁸S. M. El-Sheikh, G. C. Tabisz, and R. T. Pack, *J. Chem. Phys.* **92**, 4234 (1990).
- ¹⁹G. Maroulis, *Chem. Phys. Lett.* **312**, 255 (1999).
- ²⁰T. Bancewicz, J.-L. Godet, and G. Maroulis, *J. Chem. Phys.* **115**, 8547 (2001).
- ²¹J.-L. Godet, F. Rachet, Y. Le Duff, K. Nowicka, and T. Bancewicz, *J. Chem. Phys.* **116**, 5337 (2002).
- ²²Y. Le Duff, J.-L. Godet, T. Bancewicz, and K. Nowicka, *J. Chem. Phys.* **118**, 11009 (2003).
- ²³I. A. Verzhbitskiy, M. Chrysos, F. Rachet, and A. P. Kouzov, *Phys. Rev. A* **81**, 012702 (2010).
- ²⁴M. Chrysos and I. A. Verzhbitskiy, *Phys. Rev. A* **81**, 042705 (2010).
- ²⁵I. A. Verzhbitskiy, M. Chrysos, and A. P. Kouzov, *Phys. Rev. A* **82**, 052701 (2010).
- ²⁶J.-P. Champion, M. Loëte, and G. Pierre, "Spherical top spectra," in *Spectroscopy of the Earth's Atmosphere and Interstellar Medium*, edited by K. N. Rao and A. Weber Editors (Academic Press, New York, 1992), pp. 339–422.
- ²⁷A. R. Ravishankara, S. Solomon, A. A. Turnipseed, and R. F. Warren, *Science* **259**, 194 (1993).
- ²⁸M. K. W. Ko, N. D. Sze, W.-C. Wang, G. Shia, A. Goldman, F. J. Murcray, D. G. Murcray, and C. P. Rinsland, *J. Geophys. Res.* **98**, 10499, doi:10.1029/93JD00228 (1993).
- ²⁹W. Holzer and R. Ouillon, *Chem. Phys. Lett.* **24**, 589 (1974).
- ³⁰D. P. Shelton and L. Ulivi, *J. Chem. Phys.* **89**, 149 (1988).
- ³¹S. Montero, *J. Chem. Phys.* **79**, 4091 (1983).
- ³²W. C. Marlow, *Proc. Phys. Soc.* **86**, 731 (1965).
- ³³W. Kolos and L. Wolniewicz, *J. Chem. Phys.* **46**, 1426 (1967).
- ³⁴Y. Y. Milenko, L. V. Karnatsevich, and V. S. Kogan, *Physica* **60**, 90 (1972).
- ³⁵A. S. Pine and A. G. Robiette, *J. Mol. Spectrosc.* **80**, 388 (1980).
- ³⁶D. P. Hodgkinson and A. J. Taylor, *Mol. Phys.* **52**, 1017 (1984).
- ³⁷H. B. Levene and D. S. Perry, *J. Chem. Phys.* **80**, 1772 (1984).
- ³⁸R. Harzer, G. Schweizer, and K. Selzer, *J. Mol. Spectrosc.* **132**, 310 (1988).
- ³⁹D. McNaughton and C. Evans, *J. Mol. Spectrosc.* **182**, 342 (1997).
- ⁴⁰V. Boudon, M. Hepp, M. Herman, I. Pak, and G. Pierre, *J. Mol. Spectrosc.* **192**, 359 (1998).
- ⁴¹U. Hohm and K. Kerl, *Mol. Phys.* **58**, 541 (1986).
- ⁴²U. Hohm and K. Kerl, *Mol. Phys.* **61**, 1295 (1987).
- ⁴³W. B. Clodius and C. R. Quade, *J. Chem. Phys.* **82**, 2365 (1985).
- ⁴⁴B. J. Krohn and J. Overend, *J. Phys. Chem.* **88**, 564 (1984).
- ⁴⁵D. P. Hodgkinson, J. C. Barrett, and A. G. Robiette, *Mol. Phys.* **54**, 927 (1985).
- ⁴⁶J.-Q. Chen, F. Iachello, and J.-L. Ping, *J. Chem. Phys.* **104**, 815 (1996).
- ⁴⁷This is to be contrasted with the large values taken by constants related to stretching of the S–F bond, such as k_{133} , and with the agreement between theory [-55 cm^{-1} (Ref. 44), -56.75 cm^{-1} (Ref. 45)], and experiment [-56.25 cm^{-1} (Ref. 45)] that has been found for k_{133} .
- ⁴⁸P. P. Bera, J. S. Francisco, and T. J. Lee, *J. Phys. Chem. A* **113**, 12694 (2009). According to these scientists "Molecules possessing several F atoms will always have a large radiative forcing parameter in the calculation of their global warming potential." This is a consequence of the "linear increase in the bond dipole derivatives for the molecule, which leads to a quadratic increase in infrared (IR) intensity."
- ⁴⁹The reader should be mindful that it is the first excited state of each mode that specifies the mode's degeneracy [$n_i = g_{n_i,i}(1)$]. Note also that for the ground vibrational level of each mode, the expression of Eq. (3) gives $g_{n_i,i}(0) = 1$.
- ⁵⁰R. S. McDowell, B. J. Krohn, H. Flicker, and M. C. Vasquez, *Spectrochim. Acta A* **42**, 351 (1986).
- ⁵¹G. Herzberg, *Molecular Spectra and Molecular Structure II: Infrared and Raman Spectra of Polyatomic Molecules* (Van Nostrand Company, Toronto, 1966), Eq. (V.17).
- ⁵²It is more practical and informative, in terms of interpretation, to use a definition for the vibrational partition function in which the zero-point energy is absent. In this way $(Z_i)^{-n_i}$ becomes a probability [the probability $P_i(v_i = 0)$ that the ground-state of mode i is occupied] and $(Z_i)^{n_i}$ takes values greater than and close to 1. Parenthetically, this choice is consistent with the definition $Z_{elec} = g_{elec} \exp(D_0/k_B T)$ for the electronic partition function of SF₆, where g_{elec} is the electronic degeneracy and $D_0 = D_e - \sum_i \frac{1}{2} n_i h c v_i$ the binding energy of the molecule, the latter energy being expressed as a difference between the equilibrium energy D_e and the zero-point energy $\sum_i \frac{1}{2} n_i h c v_i$; by making this subtraction the zero-point energy has been implicitly incorporated into Z_{elec} and has thus been "removed" from the vibrational partition function.
- ⁵³S. Montero, *J. Chem. Phys.* **72**, 2347 (1980).
- ⁵⁴M. Chrysos, I. A. Verzhbitskiy, F. Rachet, and A. P. Kouzov, *J. Chem. Phys.* **134**, 044318 (2011).
- ⁵⁵M. Chrysos, I. A. Verzhbitskiy, F. Rachet, and A. P. Kouzov, *J. Chem. Phys.* **134**, 104310 (2011).
- ⁵⁶I. A. Verzhbitskiy, A. P. Kouzov, F. Rachet, and M. Chrysos, *J. Chem. Phys.* **134**, 194305 (2011).
- ⁵⁷I. A. Verzhbitskiy, A. P. Kouzov, F. Rachet, and M. Chrysos, *J. Chem. Phys.* **134**, 224301 (2011).
- ⁵⁸This behavior is to be contrasted with the one met in the recently treated^{54–57} $2\nu_3$ CO₂ overtone. There, the $2\nu_3$ overtone had been identified as the combined interaction " $(00^02) \leftarrow (00^00)$ and $(01^12) \leftarrow (01^10)$," found to include at 295 K the whole amount of the scattered intensity to proportions 92.8% and 7.2%, respectively.⁵⁶ Although, formally, some thermal factor should too have been included in those studies, the concept had not yet been revealed to us: owing to the high frequency of the CO₂ ν_3 mode (2349 cm^{-1}), $\gamma_3(295\text{ K})$ amounts to 1.00002.
- ⁵⁹The meaning of the "reduced temperature" becomes clearer after the definition $T^* = T/T_{vib}$, where $T_{vib} = h c v_i/k_B$ is the "vibrational temperature."
- ⁶⁰S. Dixneuf, M. Chrysos, and F. Rachet, *Phys. Rev. A* **80**, 022703 (2009).
- ⁶¹M. Chrysos, S. Dixneuf, and F. Rachet, *Phys. Rev. A* **80**, 054701 (2009).
- ⁶²T. D. Kolomiitsova and D. N. Shchepkin, in *Advances in Spectroscopy*, edited by R. J. H. Clark and R. E. Hester (Wiley, Chichester, 1995), Vol. 23.
- ⁶³D. A. Long and E. L. Thomas, *Trans. Faraday Soc.* **59**, 1026 (1963).
- ⁶⁴For q_1 , we have $\mu_1 = 6m_F$, with m_F the atomic mass of fluorine [see for instance L. G. Gerchikov and G. F. Gribakin, *Phys. Rev. A* **77**, 042724 (2008); see also Ref. 23; for CF₄, see Ref. 6, p. 299]. The formula $q_1 = \sqrt{\mu_1 \omega_1 / \hbar} \Delta R$ makes the link between the dimensionless normal stretch coordinate q_1 and the elongation ΔR of the S–F bond.